Building and Environment 130 (2018) 14–26

Contents lists available at ScienceDirect

Building and Environment

journal homepage: www.elsevier.com/locate/buildenv

Experimental and numerical investigations of indoor air movement distribution with an office ceiling fan

Wenhua Chen[b], Shichao Liu[a,*], Yunfei Gao[c,d], Hui Zhang[c], Edward Arens[c], Lei Zhao[b], Junjie Liu[b]

[a] Department of Civil and Environmental Engineering, Worcester Polytechnic Institute, Worcester, MA 01609, USA
[b] Tianjin Key Laboratory of Indoor Air Environmental Quality Control, School of Environmental Science and Engineering, Tianjin University, Tianjin, China
[c] Center for the Built Environment, University of California, Berkeley, CA, USA
[d] School of Architecture and Urban Planning, Guangdong University of Technology, Guangzhou, China

ARTICLE INFO

Keywords:
Ceiling fan
Blade geometry
Rotational speed
Air movement distribution
Moving reference frame
Thermal comfort

ABSTRACT

Ceiling fans provide cooling to indoor occupants and improve their thermal comfort in warm environments at very low energy consumption. Understanding indoor air distribution associated with ceiling fans helps designs when ceiling fans are used. In this study, we systematically investigate the air movement distribution in an unoccupied office room installed with a ceiling fan, as influenced by (1) fan rotational speed, (2) fan blade geometry, (3) ceiling-to-fan depth, and (4) ceiling height. We both measured and simulated air speeds at four heights in the occupied zone according to *ANSI/ASHRAE/IES Standard 55 (2013)* for seated and standing occupants. CFD predictions were validated by experimental results. In general, numerical results show that for an unoccupied space, the fan blade geometry, ceiling-to-fan depth, and ceiling height only influence air speed profiles within a cylindrical zone directly under a ceiling fan whose diameter is identical to that of the ceiling fan. However, the average speeds within the cylindrical zone at each height are very similar (< 10% in difference) for the different blade shapes studied, indicating a minor influence of blade geometries on occupants' perception of the thermal environment. The results also indicate that the velocity profile remains similar in the main jet zone (the tapered high-velocity zone under the fan blade) for various rotational speeds. The jet impingement on the floor creates radial airflow at the ankle level (0.1 m) across the room, which is not the most effective airflow distribution for cooling occupants.

1. Introduction

Energy constraints encourage the use of energy-effective electrical appliances such as ceiling fans to achieve indoor thermal comfort, especially in developing countries (e.g., China and India) and regions with mild and warm climates. Ceiling fans accounted for approximately 6% of residential electricity consumption in India in 2000, which might increase to 9% in 2020 [1].

Elevated air speeds from ceiling fans can offset the need for low thermostat cooling set-points, and provide occupants with enhanced thermal comfort at a lower energy consumption. *ANSI/ASHRAE/IES Standard 55 (2013)* [2,3] recommends an elevated air movement method to maintain thermal comfort in the occupied zone at increased indoor temperature. Airflow from a ceiling fan with a speed between 0.5 m/s and 1.0 m/s compensates for approximately 3 K indoor temperature increase [4] or even more [5]. Energy simulations suggest a saving of 15% residential cooling energy by using ceiling fans and a thermostat set-up of only 1.1 K [6], saving between 17% and 48% for 400 Florida households [7]. Additional simulations show that in commercial office buildings, a 1 K setpoint extension is associated with about 10% HVAC energy savings in most types of climate [8].

1.1. Ceiling fan evaluation approaches

The performance of ceiling fans is often evaluated from the perspective of energy consumption for created airflow rates [9–11]. Overall, a ceiling fan that provides a certain airflow rate at a lower power input is rated with a higher efficiency. The American Energy Star program defines the minimum efficacy levels for certified ceiling fans. For instance, fans at a low speed must have a minimum airflow rate of 2124 m^3/hr and an efficiency of 263 m^3/hr/W [10] A nice summary of the ceiling fan energy efficiency evaluation methods is presented by de la Rue du Can et al. [1]. However, such performance evaluation does not consider air movement distribution within the room, which is the feature that affects occupants' thermal comfort.

Schiavon and Melikov [12] developed a cooling-fan efficiency (CFE)

* Corresponding author.
E-mail address: sliu8@wpi.edu (S. Liu).

https://doi.org/10.1016/j.buildenv.2017.12.016
Received 1 October 2017; Received in revised form 30 November 2017; Accepted 15 December 2017
Available online 18 December 2017

index to assess the performance of cooling fans, including ceiling fans, by considering the reduction of equivalent temperature that is caused by elevated air movement when compared to an environment with still air. The CFE is defined as the ratio of cooling effect to fan power. This method combines the factors of both the energy saving and thermal comfort rather than pure airflow capacity. Based on the comfort with elevated air movement described in the *ANSI/ASHRAE/IES Standard 55 (2013)* [2], the CFE index relies on the room air distribution to provide thermal comfort at any given point.

A new ASHRAE Standard 216 (ceiling fan method of testing) is currently under development to quantify and to predict airflow under ceiling fans. To evaluate fan performance, the existing indexes focusing on energy efficiency and airflow volume might not be enough. An index is also needed that links fan speed to the distribution of air movement in the occupied zone, since that determines occupant thermal comfort. This second index is included in the goals of ASHRAE Standard 216. A final goal of the Standard is a design tool to provide guidance for designers when ceiling fans are applied. For the latter two goals, understanding air movement distribution in a room is a key component. This team performed activities to support the ASHRAE Standard 216 effort. First, detailed laboratory measurements of occupied zone air speeds, with and without furniture, have been taken under a single ceiling fan. The detailed measurements profiles are described [13].

1.2. Factors affecting air flow distribution by ceiling fans

Most fan studies have focused on the air flow volume induced by ceiling fans, but not on the room air movement distribution, and particularly not on the distribution in the occupied zone. Laboratory [14,15] and field [16] studies compared energy efficiency index and indoor airflow distributions from different fan speeds and blade diameters. The studies indicated that the vertical temperature difference decreases with increasing fan speed, and that wider fan blades increase airflow coverage with increased energy efficiency [16], and that fans with a larger diameter and lower rotation speed reduce noise [17]. There are a few studies that examine the effect of air speed on bacterial removal [18–21], all finding that increasing speed results in higher disinfection efficacy. These studies did not examine the air movement distribution in the occupied space.

There has been considerable effort to improve the design of the fan blades in order to increase the flow volume, uniformity along the fan radius, and to increase the air movement coverage area. Adeeb et al. [22] focused on the number of blades and found that increasing the number of blades resulted in a higher flow volume. Afaq et al. [23] measured the effect of rake angles on the flow volume and found that a 6° upward rake angle (fan blades tilted above the horizontal level) provided the highest flow volume. Jain et al. [24] found that introducing winglets and spikes on the blade tip increased flow volume.

Volk [25] designed aerodynamic attachments as auxiliary blade attachments wedged onto the trailing edges of the main blades of conventional ceiling fans. Bird [26] designed a positive twist adjacent to the rotor end of the blade, so that blade pitch increases from a tip end of the blade to the rotor end of the blade. Sonne & Parker [16] developed twisted and tapered blades with airfoil cross-section. The twisted, tapered blades increase airfoil efficiency by reducing energy lost to wingtip turbulence and flow separation. Parker published several patents [27–29] about the blade shape, providing the basis for the “Gossamer Wind” fan. Schimidt and Patterson [9] evaluated the power consumption/airflow power of ceiling fans with an axial flux brushless DC motor. The fan blades were reshaped aerodynamically to provide a more constant air velocity across the area below the blades.

Additionally, laboratory measurements [30] indicated that a ceiling surface began to reduce fan flow volume only when the distance between the ceiling and the fan (diameter is 1.4 m) is 0.4 m or less.

1.3. CFD models

Numerical simulation using CFD has been successfully applied in ventilation and indoor air distribution research [31–33]. All the reviewed work used Reynolds-averaged Navier-Stokes equation (RANS) models because of their less computational requirements compared to Large Eddy Simulation (LES) and Direct Numerical Simulation (DNS) [34,35]. Momoi et al. [30] compared the standard k-ε turbulence model and the Reynolds stress model (RSM) in a study of turbulence models used in ceiling fan simulations. The comparisons indicated unremarkable differences between the two models.

Because of the complexity of ceiling fan’ geometries, it is generally cost-prohibitive to directly model a rotating ceiling fan using the moving mesh method [36,37]. Instead, the body force model (also called momentum method) and multiple reference frame (MRF) method are often applied [36,38]. Bassiouny et al. [39] fitted the previous measured data [24] as Dirichlet-type boundary conditions based on the body force model, and predicted the airflow induced by a ceiling fan using the standard k-ε model. Zhu et al. [19] used MRF together with the realizable k-ε model to examine the ceiling fan-driven flow in an environmental chamber. Contrary to these, Babich et al. [38] concluded that SST k-ω model is better than the standard k-ε and realizable k-ε models when applying the body force model to ceiling fan simulations. However, the conclusion was drawn when the ceiling fan was simulated by a body force model rather than MRF.

We identified the following limitations of previous related studies. First, the possible effects of fan blade geometries on airflow patterns have not been thoroughly investigated. The challenges of considering fan blade geometries in CFD simulations entail investigations into how much air distribution varies with different fan geometries. Second, even if previous studies have recognized that using ceiling fans is an energy-efficient solution for thermal comfort via air movement elevation, many factors, such as fan rotational speed and installation height, could influence air distribution and thermal environment in the occupied zone. Insufficient guidance about these factors inhibits designers and practitioners from applying ceiling fans properly in practice. Finally, turbulent jets usually display the properties of self-similarity in the self-preservation region (further down from the initial development region close to the fan blades) where the flow profiles are self-similar [40]. We hypothesize that similar self-similarity might exist for the primary airflow induced by a ceiling fan. Nevertheless, we could not find such an investigation in the literature.

1.4. Objectives

This paper aims to provide fundamental knowledge on how fan properties and room configuration affect the air movement distribution in an office room. In particular, the present study systematically investigates the influences of (1) ceiling fan rotational speed, (2) fan blade geometry, (3) distance between ceiling and fan, and (4) ceiling height on air distribution in an unoccupied office, using computational fluid dynamics (CFD) simulations. The CFD simulations were first validated by laboratory experiments and then applied to investigate these factors.

2. Methodology

2.1. Baseline experimental data

Simulations in this study are based on a previous experimental study of an office room conducted at the Center for the Built Environment (CBE) at University of California, Berkeley [13]. The room had geometries of 5.5 (X) × 5.5 (Z) × 2.5 (Y) m, as shown in Fig. 1a. A ceiling fan (Haiku 60, Big Ass Fans, Inc.), 1.5 m in diameter, was installed at 0.2 m below the ceiling surface. Fig. 1b is a snapshot of the fan used in the experiment. Smoke visualization was used to ensure that the room

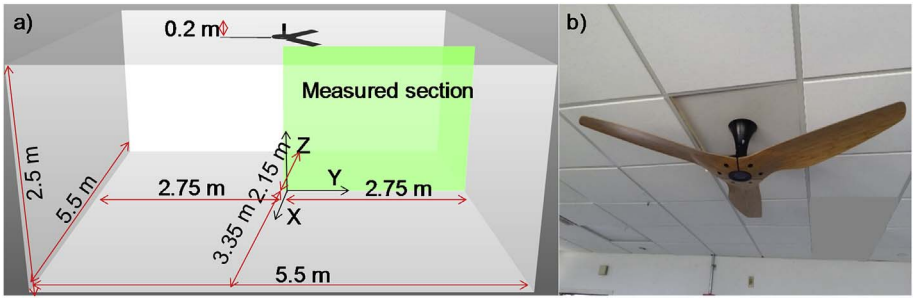

Fig. 1. Experimental setup. a) Schematic of the office room; b) Haiku ceiling fan.

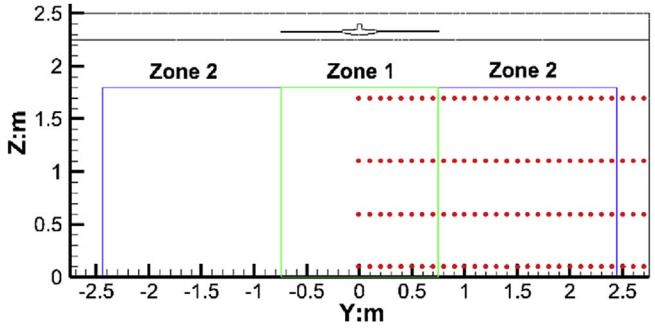

Fig. 2. Measurement points for three rotational speeds (72 rpm, 124 rpm, and 182 rpm).

walls have negligible effects on the airflow generated by the fan.

In order to better describe flow characteristics, we divided the occupied zone into two regions, Zone 1 and Zone 2. As shown in Fig. 2, Zone 1 is the cylindrical zone, with the same diameter (1.5 m) as the fan, right below the fan blades, and the remaining area in the occupied zone is Zone 2 (the occupied zone refers to the space from the floor and 1.8 m above the floor and more than 0.3 m away from internal walls, as defined in *ANSI/ASHRAE/IES Standard 55 (2013)* [2]).

Due to the symmetry of air velocity distribution below the ceiling fan, we measured the velocity magnitude over a half of a vertical plane (the green plane in Fig. 1a) intersecting with the center of the fan. We used omnidirectional anemometers to measure air speeds at a sampling frequency of 0.5 Hz. The anemometer system, manufactured by *Sensor Inc.*, is designed for the typically low air speeds of room flow with an accuracy ± 0.02 m/s or 1% of reading (0.05–5 m/s). For each location, we measured air velocity for a period of 3 min. We measured air speeds at four locations in total for eight heights in the occupied zone [13]. Since the thermal environment at four heights (0.1, 0.6, 1.1 and 1.7 m) is often applied to evaluate occupants' thermal comfort for seated and standing occupants [2], this study uses air speeds at only the four heights above the floor as shown in Fig. 2 (blue box represent Zone 2). The measurements at each height consisted of 28 locations, every 0.1 m from the center of the ceiling fan.

The fan was operated at three rotational speeds, 72 rpm (revolutions/minute), 124 rpm, and 182 rpm, according to three fan speed settings.

2.2. Numerical simulation

We simulated three ceiling fans with different blade shapes to examine how airflow distribution is affected. The geometries of the three fans (Fig. 3a–c) were obtained from a free CAD library [41]. They are the only available digital fan models having three blades, and they represent fans that are commonly available in the market. There was no digital description of the Haiku plywood-bladed fan (Fig. 3d) for which the laboratory velocity measurements had been obtained. We therefore measured the Haiku airfoil parameters at four equally spaced stations (Table 1), and obtained the comparable parameters from the three digital fan models using SolidWorks, exporting to Gambit 2.4.6 for meshing. The diameters of these four ceiling fans are identical, 1.5 m. The blade thickness is roughly constant in each fan, between 4 and 5 mm.

In order to get a high-quality computational mesh, the computational domain was divided into two parts, a rotating reference frame around the ceiling fan and the rest region. After a range of trial simulations considering the size of the rotating domain proposed by literature [42,43], we applied a rotating reference frame with a diameter of 2.0 m and a height of 0.17 m (0.12 m above and 0.05 m below the ceiling fan). The mesh in the rotating reference frame consisted of tetrahedral and hexahedral grids (Fig. 4). The grids outside of the rotating reference frame were hexahedral to save computational resources. We conducted a grid independence test with three mesh sizes (2.4 million, 4.1 million, and 6.0 million) by comparing simulated airflow accordingly. The test results indicated that a mesh with 4.1 million grids generated insignificant difference when compared with a finer mesh, 6.2 million grids. Fig. S1 in the supplementary information shows the comparison in detail. Consequently, we employed the medium grid number (approximately 4.1 million) for all simulations in this paper. The rotating reference frame accounts for 37% of the total grids to capture air dynamics around the ceiling fan. We optimized the mesh in Gambit and ensured the skewness of the grids less than 0.86. The y^+ values on the walls of the ceiling fan range from 3 to 25 that is suitable for standard wall functions. The growth rate of cell-size is small than 1.2. The aspect ratio is less than 6.2.

We applied the multiple reference frame (MRF) model to simulate the rotating motion of ceiling fans. The rotating wall surfaces were treated as stationary boundaries relative to the rotating frame. When the equations of motion were solved in this rotating reference frame, the acceleration of the fluid was supplemented by additional terms that appear in the momentum equations. MRF is normally used for steady-state conditions [20,44], with the dynamic mesh method often used for transient state conditions. However, the high computational cost of dynamic mesh has not been found to give significant improvement in airflow prediction [36]. We used the standard k-ε model in this study, as various researchers have found that the model provided a reasonable estimation of the overall trend of airflow in terms of parameters such as pressure and velocity, when the MRF approach was used to simulate a ceiling fan [20,44]. For this investigation, the SIMPLE algorithm was applied for the pressure coupling as it contains a slightly more conservative under-relaxation value of up to 0.8. Without heat sources in the room, the numerical solutions were solved in the isothermal condition with a second-order approximation. We used standard wall functions for all wall boundaries. Rotational velocity was assigned to wall boundaries for fan blades. Table 2 describes the simulated cases in this study.

3. Results

3.1. Validation of numerical modeling of a ceiling fan

As depicted in Fig. 5, the numerical velocity profiles of fan1 at four heights (0.1 m, 0.6 m, 1.1 m, and 1.7 m) are compared with measured

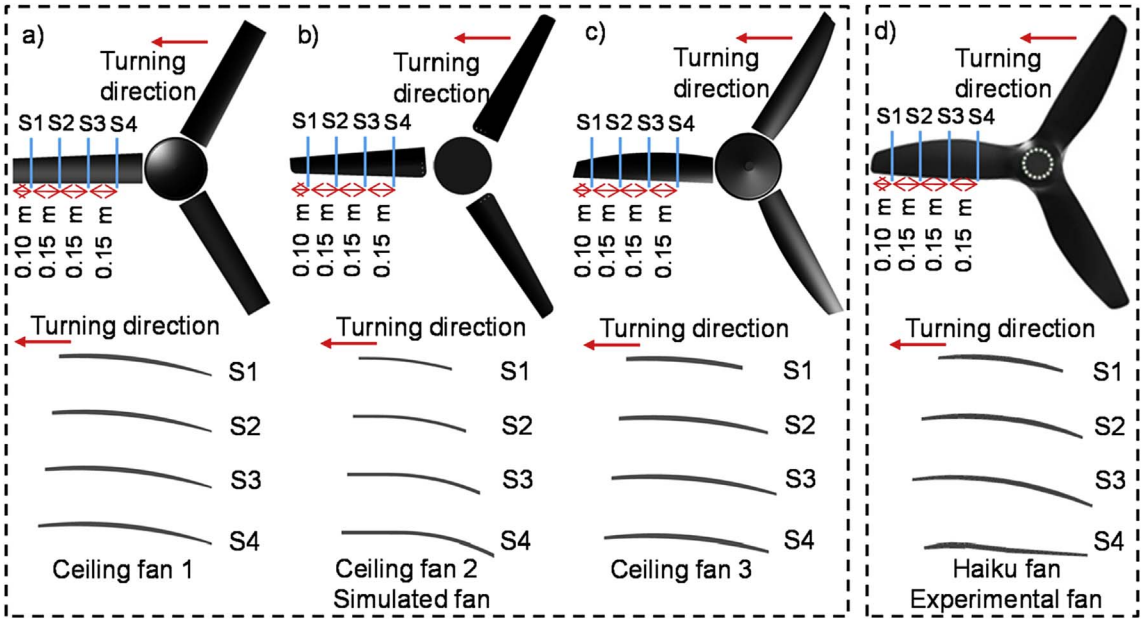

Fig. 3. Ceiling fan geometry and blade shapes: a) ceiling fan 1; b) ceiling fan 2; c) ceiling fan 3; d) Haiku fan.

data from the office room with the Haiku ceiling fan (Fig. 3) [13]. The ceiling fan-driven flow is generally well-predicted by CFD modeling. The velocity profiles for the four heights are all well represented by the CFD predictions. As shown in Fig. 5a–d, the differences mainly happen near the fan axis (Zone 1, width same as the fan diameter, shaded with grey in Fig. 5). These discrepancies might be attributed to the geometry difference between ceiling fans. As shown in Fig. 3a and d, the diameter of the Fan 1 hub is larger than that of the Haiku hub. This may explain the difference between the simulated and measured velocities at 1.7 m (Fig. 5a), where the peak happens closer to the fan center in the measured Haiku than the simulated Fan1. Besides, Haiku blade is wider and has more curvature than the Fan1 (Table 1) and appears to push the air flow outward slightly more than the simulated, as the air moves down towards the floor, (seen in Fig. 5b and c for comparisons at 1.1 m and 0.6 m heights). To quantify the uncertainties of simulated air speeds at different heights, the normalized root-mean-square deviations (NRMSDs) were calculated,

$$NRMSD = \sqrt{\left(\sum_{i=1}^{n}(V_{sim,i} - V_{exp,i})^2\right)/n} \Big/ (V_{sim,max} - V_{sim,min})$$

where i refers to a measured location at a certain height, and n is the total number of the locations. The symbols *sim* and *exp* represent simulation and experiment, respectively.

The maximum difference occurs at the height of 0.6 m with a value of approximately 19.3%. The velocity profiles in Zone 1 between the measured and simulated are very close. The CFD models predict velocities accurately in Zone 2. The differences between the predicted and the measured velocities tend to reduce when the location is further away from the fan axis. The results suggest that the ceiling fan-driven flow can be predicted by the combination of Standard k-ε model with the Multiple Reference Frame (MRF) fan model.

3.2. Influence of rotational speed

Fig. 6 depicts the measured air velocity profiles at four heights for

Table 1
Parameters of fan blades.

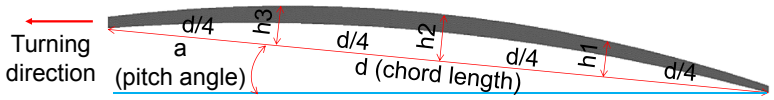

	Fan 1	Fan 2	Fan 3	Haiku		Fan 1	Fan 2	Fan 3	Haiku
	S1					S3			
d (mm)	137.2	80.0	98.9	127	d (mm)	149.3	114.5	140.0	185
h1 (mm)	6.9	4.1	6.2	4	h1 (mm)	8.5	8.2	8.0	7.5
h2 (mm)	9.2	4.8	7.0	5	h2 (mm)	10.7	9.5	9.9	11
h3 (mm)	7.9	4.3	6.5	4	h3 (mm)	9.0	6.8	8.3	8
a (°)	6.7	6.7	4.3	6.1	a (°)	6.1	7.9	5.4	8.39
	S2					***S4***			
d (mm)	143.2	97.6	126.7	165	d (mm)	155.3	131.9	146.2	166
h1 (mm)	7.6	6.4	7.1	7	h1 (mm)	8.4	10.8	8.1	0
h2 (mm)	9.5	7.7	8.7	9	h2 (mm)	10.8	12.4	10.2	0
h3 (mm)	8.0	5.9	7.6	6.5	h3 (mm)	8.9	8.2	8.6	4
a (°)	6.6	7.2	5.3	6.6	a (°)	5.7	8.4	4.8	2.7

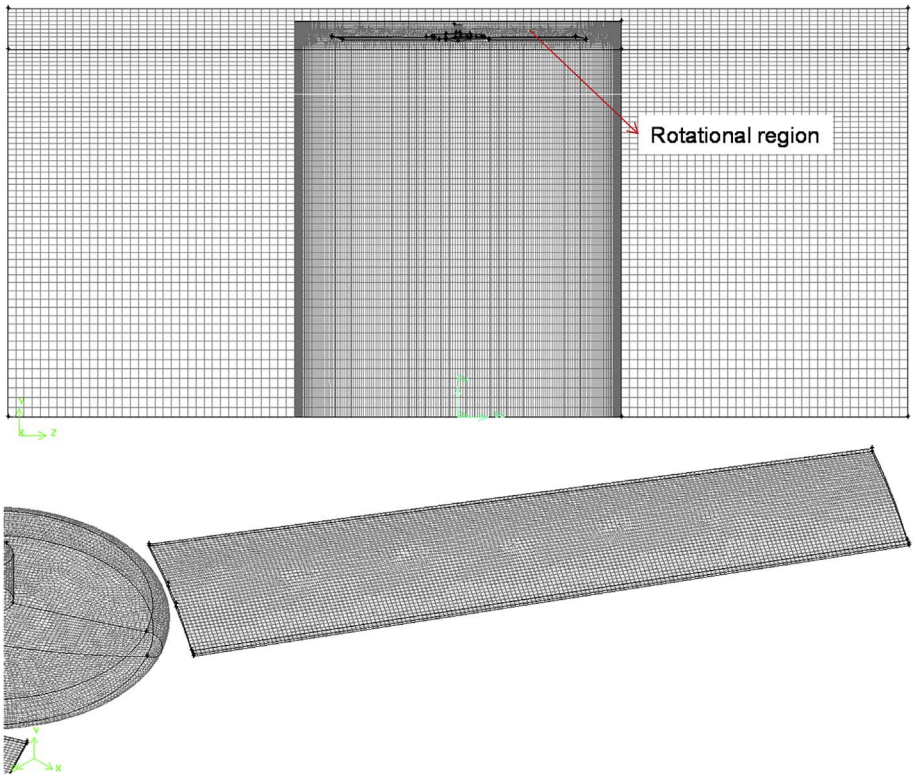

Fig. 4. Mesh for indoor airflow simulation with a ceiling fan.

Table 2
Description of simulated cases.

Factor	Cases setup	Notes
Fan blade geometry	Fan 1, Fan 2, and Fan 3	Rotational speeds were slightly different to ensure the same airflow rate for the three different fans (Fan 1–115 rpm, Fan 2–135 rpm, and Fan 3–130 rpm); Ceiling-zone depth: 0.2 m; Ceiling height: 2.5 m
Ceiling-zone depth (distance from fan to ceiling)	0.15, 0.2, 0.25, 0.3, and 0.35 m	Fan 1; Rotational speed: 115 rpm; Ceiling height: 2.5 m
Ceiling height	2.5, 3.3, and 4 m	Fan 1; Rotational speed: 115 rpm; Ceiling-zone depth: 0.3 m

the Haiku ceiling fan at 72, 124, and 182 rpm. Spatial-average velocity in the occupied zone is increased with the increase of rotational speed. There is a peak velocity in the Zone 1 (shaded zone in Fig. 6) for each height even at the lowest rotational speed, except for the level at 0.1 m. Air speed at the ankle level (0.1 m) is significantly elevated almost across the entire room. In the regions beyond Zone1, air velocity at the ankle level is even greater than that at other three heights. Fig. 6b shows that air speed at 0.1 m exceeds 0.5 m/s when the ceiling fan is operated at a medium speed, which could cause draft at occupants' lower legs and ankles if the ambient temperature is not warm [45].

For the rotational speed of 72 rpm, the locations of peak velocity shift outwards from the ceiling fan hub with the decrease of height, which indicates that airflow spreads slightly outwards when moving down. For the other two rotation speeds (124 and 182 rpm), the locations of these peak velocities at each height (except 0.1 m) happened at

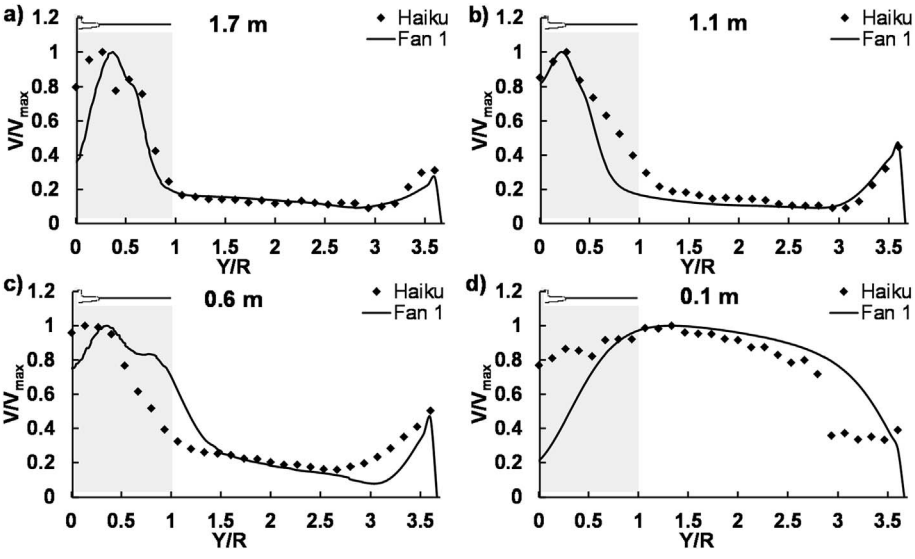

Fig. 5. Comparisons between the experimental and numerical air velocity profiles at different heights: a) Y = 1.7 m, b) Y = 1.1 m, c) Y = 0.6 m, d) Y = 0.1 m.

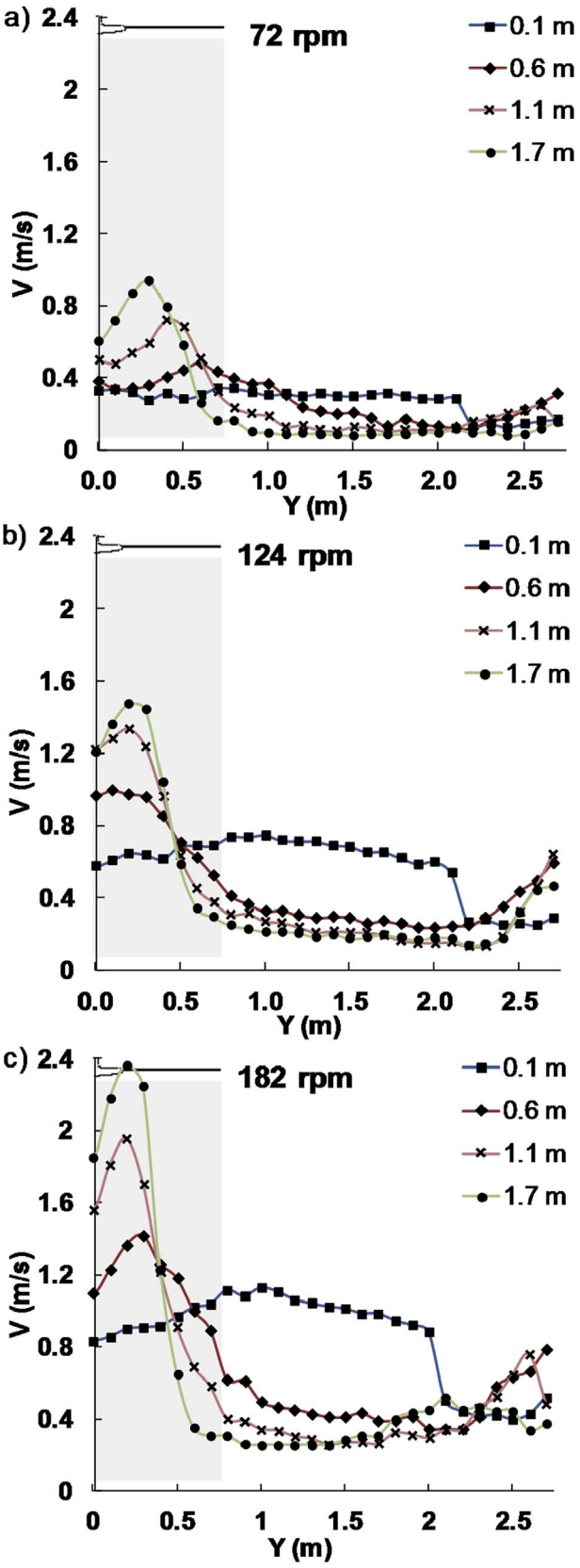

Fig. 6. Airflow performance of the Haiku ceiling fan at different rotational speeds. a) 72 rpm; b) 124 rpm; c) 182 rpm.

approximately 0.5R (radius of the ceiling fan: 0.75 m) horizontally from the ceiling fan hub. In addition, when the airflow approaches a wall, air velocity rises in the region near the wall due to the pressure created by upward circulated flow, which was also observed by Jain et al. [24].

In Fig. 7, we normalized air velocity profiles using the maximum (peak) velocity (V_{max}) at the corresponding heights. All dimensionless velocity ratios in Fig. 7a follow a similar profile at the height of 1.7 m. The peak velocity of each speed occurs at approximately 0.5R (fan radius) horizontally away from the fan hub. At the heights of 1.1 m (Fig. 7b) and 0.6 m (Fig. 7c), as described in Fig. 6, the self-similarity can be achieved for only high rotational speeds, such as 124 rpm and 182 rpm, not the low rotational speed, 72 rpm. The peaks for the 1.1 m and 0.6 m with the 72 rpm moved outwards. Since the axial component pushes air downwards while the acceleration components, which are added as source terms into the momentum equations for all the volume that is driven by the fan blades, generates rotational movement, this phenomenon could be illustrated by the reason that the axial component is reduced while the theta component (tangential velcotity) is relatively increased at a low rotational speed or further down away from the fan. Hence, the similarity of the vertical downward jet profiles generated is broken by the relatively increasing influence of the tangential velocity. The results suggest that velocity self-similarity can be achieved at only high rotational speeds. The critical rotational speed might depend on the blade geometry and size.

3.3. Effect of fan blade geometry

Fig. 8 shows simulated airflow patterns in the measured section with three different fans (Fig. 3). The sectional views of airflow created by the three ceiling fans illustrate a similar airflow pattern in the measured section. In Fig. 8, vortexes are generated at the tip of fan blades. A ceiling fan entrains airflow by producing negative pressure above the blade, and drives the flow as a swirling jet that impinges on the floor.

The biggest differences among the three flow profiles are probably the horizontal coverage of the high-speed range (represented by colors excluding blue). The differences might be attributed to the geometry blade difference between ceiling fans. The main geometry differences between the three fans are that 1) Fan 1 has slightly wider blade than Fan 2; 2) the Fan 2 blade becomes narrower towards the blade tip; and 3) Fan 3 has a similar blade width as the Fan 1, but is curved (Fig. 3). The shape of the Fan 2 may not spread the air as much as the other two. That is what we see in Fig. 8 where the high-velocity zone is narrower for Fan 2. However, the differences are small and probably negligible.

In Fig. 9, we normalized air velocity profiles by the maximum velocity (V_{max}) at the corresponding heights, and the radial distance (Z) from the fan center by the fan radius (R), for the rotation speeds listed in Table 2, around 124 rpm. The four figures in Fig. 9 compare the normalized velocity profiles for the data from the three simulated fans and the measured data from the Haiku fan at four heights. In general, fan blades have a significant effect on the velocity distribution only in Zone 1, directly below the ceiling fan. The positions of peak velocity are different for four fans at four heights. However, the average (or the integrated) velocities in Zone 1 are very close for the four fans. The difference is diminished in the region outwards ($Z/R > 0.5$). This is discussed in more detail in the discussion section.

Fig. 9b also compares the normalized velocity profiles with measured data from four ceiling fans by Sonne and Parker [16] at only $Z = 1.1$ m since the literature does not report velocity at other heights. It should be noted that fan A and fan B have five blades, and fan C and fan D have four blades. The diameters of all the four fans are 1.32 m, but unfortunately, they [16] did not mention their shapes in detail. In spite of differences in the blade number, diameter, and the fan shapes, the comparison of dimensionless velocity profiles of the eight ceiling fans (measured and simulated) in Fig. 9b suggests that self-similarity of velocity could be reasonably obtained with the normalized radial distance. However, differences do exist. As air speed decays with height, the swirling effect due to the revolving fan becomes comparable with the downward flow momentum. Therefore, the shape of ceiling fan

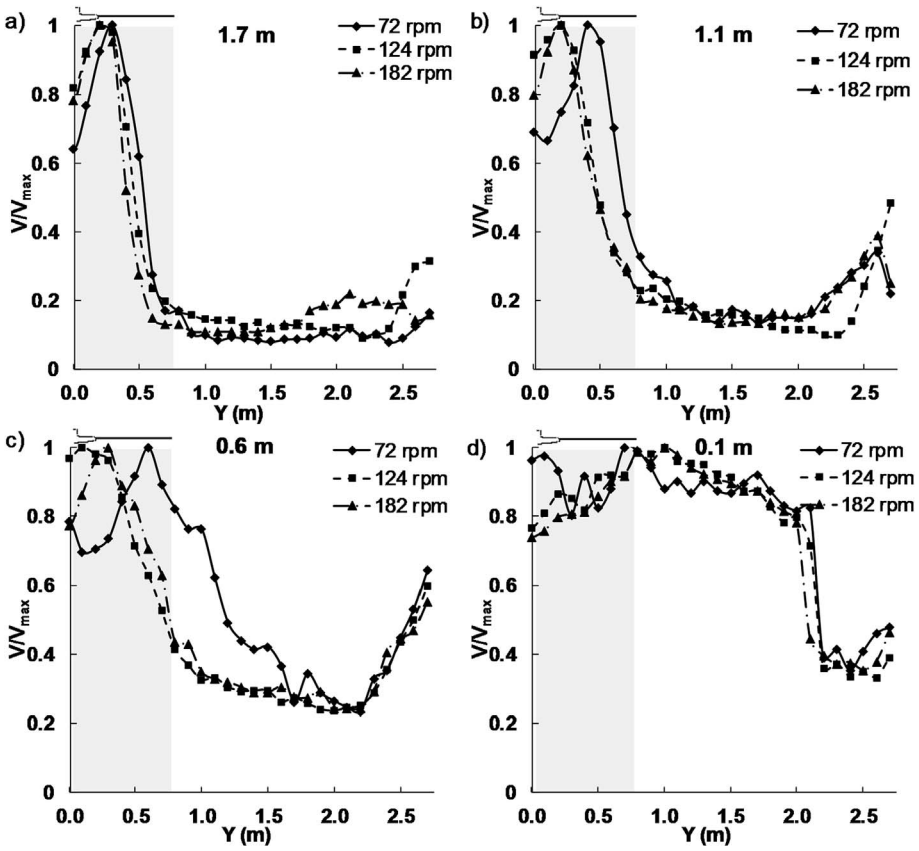

Fig. 7. Velocity similarity of ceiling-fan driven airflow. a) Y = 1.7 m, b) Y = 1.1 m, c) Y = 0.6 m, d) Y = 0.1 m.

blades appears to have a considerable influence on airflow pattern. As depicted in Fig. 9c, the difference of normalized velocity profiles among Fan 1–3 is remarkable and cannot be ignored at $Z/R < 1.5$. In addition, airflow stagnates close to the room floor and moves radially along the floor where the revolving effect decays. Fig. 9d displays that normalized speed follow a similar profile for the three fans when $Z > R$.

3.4. Influence of distance between fan and ceiling

A ceiling fan draws in room air through the space between the fan and the ceiling. Too little depth in this space increases flow resistance and may reduce airflow rate and air speed below the fan (too much resistance 'starves' the airflow into the fan and reduces the flow below). Fig. 10 shows air speed profiles with five distances between the fan and the ceiling (D = 0.15, 0.2, 0.25, 0.3 and 0.35 m).

Fig. 10a–c shows that air speed profiles vary primarily in Zone 1. The peak air speeds in Zone 1 at 1.7 m are not decreased substantially by the fan-to-ceiling distance. The peak and average air speeds at 1.1 m and 0.6 m reduce significantly when the fan-to-ceiling distance is smaller than 0.3 m for the given rotational speed. This difference between 1.7 m, 1.1 m and 0.6 m suggests a reduced axial velocity component and relatively increased radial velocity component further from the fan. Air speeds at the height of 0.1 m (Fig. 10d) do not vary considerably, which might be attributed to the effect of the floor. Since the air reached the floor and turned into a horizontal flow, the vertical momentum decayed sharply and formed a horizontal jet zone within a narrow range. The air speeds at 0.1 m are influenced less by the ceiling fan than the floor, resulting in different velocity profiles compared to

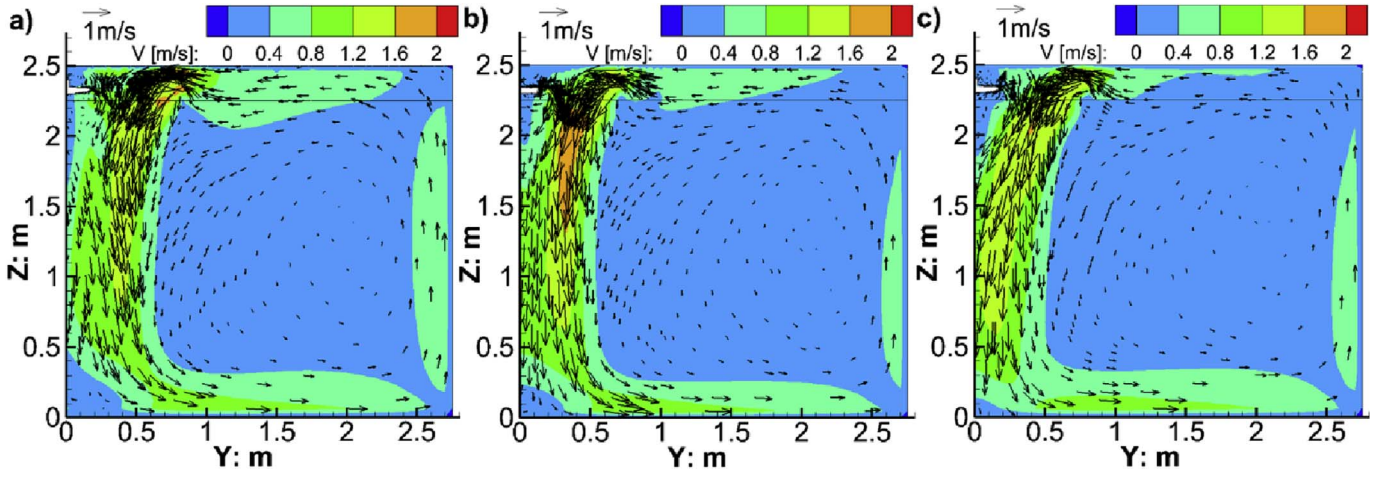

Fig. 8. Comparison of simulated airflow patterns in the room with different ceiling fans (Fan diameter 1.5 m): a) Fan 1; b) Fan 2; c) Fan 3.

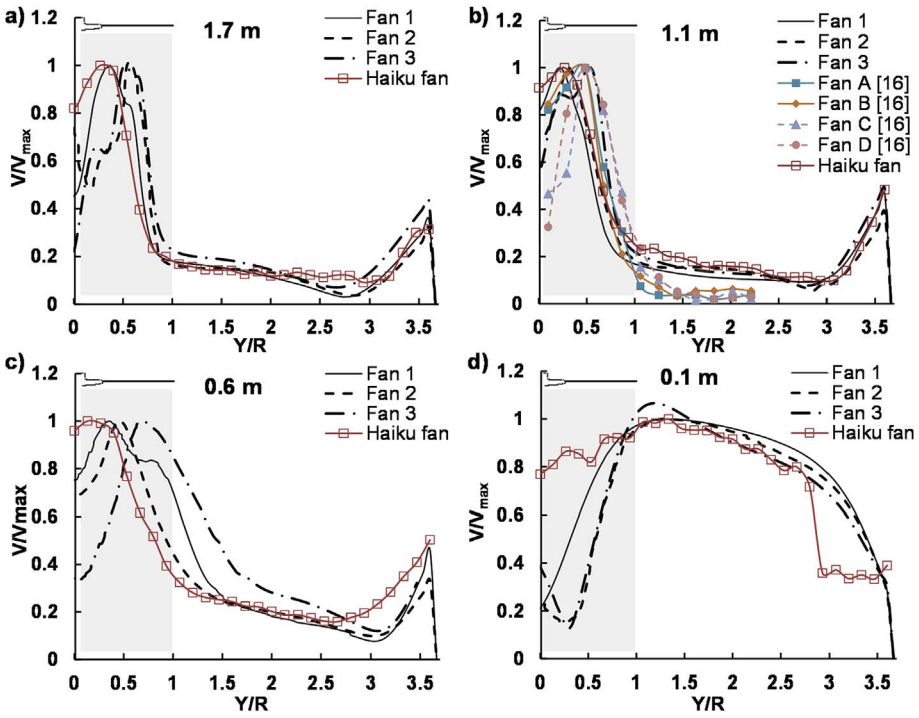

Fig. 9. Comparison of simulated velocity profiles in the room with different ceiling fans at a) 1.7 m, b) 1.1 m, c) 0.6 m, d) 0.1 m. Rotational speeds: Fan1 (115 rpm), Fan 2 (135 rpm), Fan 3 (130 rpm), Fan A (105 rpm), Fan B (103 rpm), Fan C (97 rpm), Fan D (120 rpm), Haiku ceiling fan (124 rpm).

other heights. We will discuss the average air speed in Zone 1 for various fan-to-ceiling distances later in the discussion section.

3.5. Effect of the ceiling height

In this part, three typical ceiling heights (H_1 = 2.5 m, H_2 = 3.3 m, H_3 = 4.0 m) are discussed to determine the influence of the ceiling height. The distance between the ceiling and fan is fixed at 0.2 m. Fig. 11 presents a comparison between velocity vectors of these cases at 115 rpm in the middle section of the room. The airflow patterns are almost identical to that depicted in Fig. 8. However, the velocity magnitudes decay with the increase of ceiling height owing to the reduced momentum at the same level above the floor.

Fig. 12 compares the simulated air speed profiles for the three different room heights. In Zone 1, the peak air speeds vary slightly for room heights of 2.5 m and 3.3 m at 1.7 m and 1.1 m, but much closer when compared to the peak air speed for the room height of 4 m (Fig. 12a and b). The reason might be that the 1.7 m level for the two ceiling heights (2.5 m and 3.3 m) is located in the jet potential core region where air speeds decay marginally. The 1.7 m height might be outside of the potential core region when the ceiling height is 4 m, and therefore decays more obviously. As air travels towards the floor, it

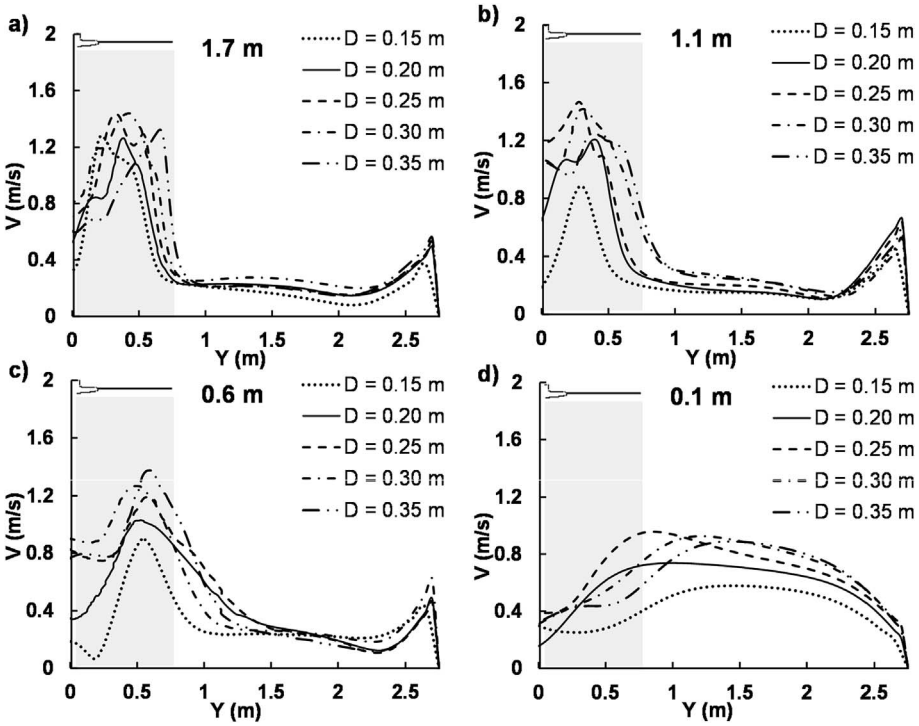

Fig. 10. Comparison of velocity components in various locations with different distances between the fan and the ceiling (115 rpm): a) 1.7 m, b) 1.1 m, c) 0.6 m, d) 0.1 m.

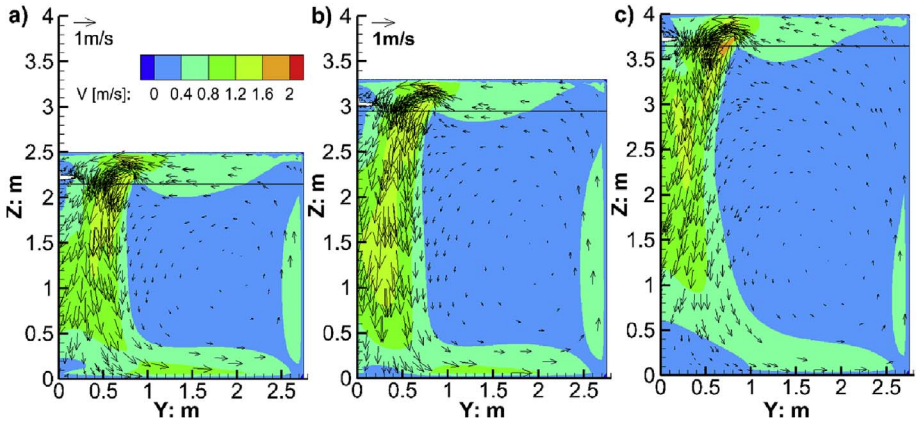

Fig. 11. Comparison of velocity distribution with different distance (Fan: Ceiling fan1; Rotational speed: 115 rpm; Distance between ceiling and fan: 0.3 m).

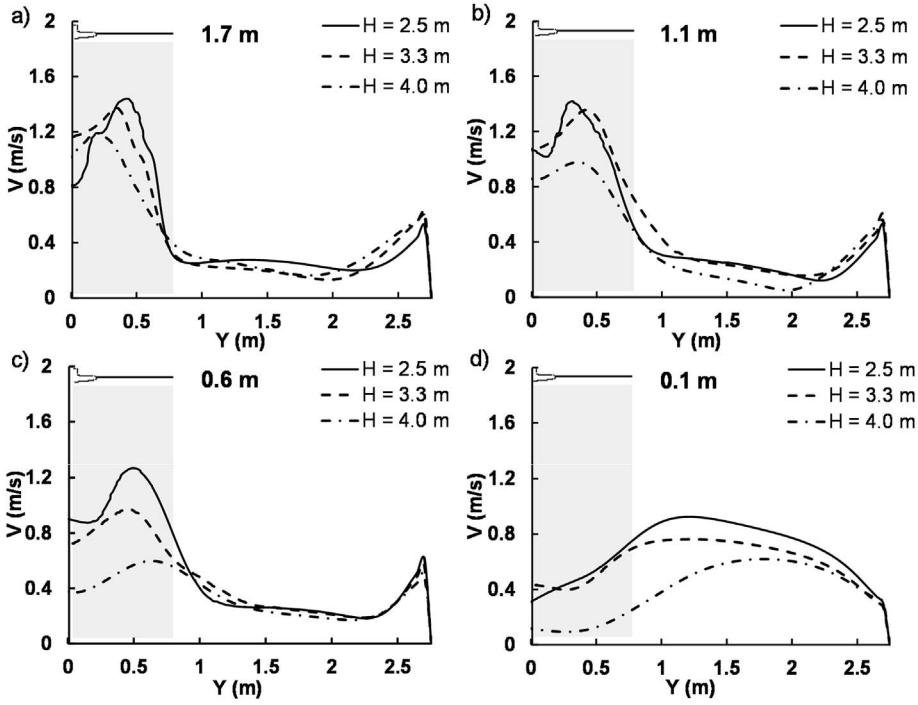

Fig. 12. Comparison of velocity components in different locations with different distance (Fan: Ceiling fan1; Rotational speed: 115 rpm; Distance between ceiling and fan: 0.3 m).

spreads more. Therefore, the magnitudes of the air speeds at the 0.6 m and 0.1 m are much smaller for the 4 m ceiling height than the other two. The influence of the ceiling height on air speeds will reduce with the horizontal distance from the fan. For example, the difference in the Zone 2 is much smaller when compared to Zone 1 under the fan. In general, Fig. 12 indicates that an elevated ceiling height decreases air speeds in the occupied zone directly under the ceiling fan.

4. Discussion and limitations

4.1. Average air speed in Zone 1

As shown in the "Results" section, air speed created by a ceiling fan varies greatly in a narrow cylindrical region under the fan. Because a person experiences fan speed not at a point, but the air speed over an area, for designing typical office ceiling fans (e.g., 1.5 m in diameter), we believe that information about the average air speed in the cylindrical region at each height is more practical and helpful than air speed profiles. Table 3 summarizes the average air speeds in Zone 1 of all the investigated scenarios at four heights (1.7, 1.1, 0.6, and 0.1 m). It also lists the percentage of difference in average speeds caused by various factors, compared with the corresponding reference conditions (marked in the table).

Table 3 shows that the rotational speed and ceiling height have a stronger effect on the average air speed in Zone 1 than does the blade geometry, or the distance between fan and ceiling. Average air speeds are increased with the rotational speed. The ceiling height is an important factor for average air speed in the occupied zone. In a typical office environment, with the ceiling height being increased from 2.5 to 3.3 m, the maximum average air speed reduction is 20% (happening only at the 0.6 m height; the reduction is 4% for all the other heights) when the rotational speed is 115 rpm and the distance between ceiling and fan is 0.3 m. However, the reduction can reach 54% when the room is 4 m high. Care needs to be taken when designing a high space room as air speed in the occupied zone is significantly reduced. Fans with a bigger size or longer down-rods are applied in such spaces to offset this.

Even if air speeds vary greatly among different blade geometries when $Z/R < 0.5$ (Fig. 9), the average air speeds under the ceiling fan are almost identical (relative difference smaller than 5%) for each of the four heights, Z = 1.7, 1.1, 0.6 and 0.1 m. The result indicates that the blade geometries simulated have little effect on the average air velocity under the ceiling fan. Furthermore, the average air velocity in Zone 1 increases with increasing distance between fan and ceiling (from 0.2 to 0.35 m) for Z = 1.1, 0.6 and 0.1 m. The maximum increase (37%)

Table 3
Comparison of average air velocity in Zone 1 (under the fan blades) in the occupied zone.

Factors	height (m)	Average air velocity in Zone 1 (m/s)				Relative difference (%)			
Rotational speed		***60 rpm***	***115 rpm***	***180 rpm***	-	***60 rpm***	***115 rpm*** *	***180 rpm***	-
(rpm)	1.7	0.61	0.95	1.37	–	−36	ref	44	–
(Fan 1)	1.1	0.54	0.92	1.29	–	−41	ref	40	–
	0.6	0.10	0.81	1.19	–	−51	ref	46	–
	0.1	0.31	0.65	0.83	–	−52	ref	28	–
Blade geometry		***Fan 1***	***Fan 2***	***Fan 3***	-	***Fan 1*** *	***Fan 2***	***Fan 3***	–
(115 rpm, 0.2 m fan-to-ceiling distance)	1.7	1.01	1.01	0.98	–	Ref.	0	−3	–
	1.1	0.94	0.89	0.90	–	Ref.	−6	−4	–
	0.6	0.81	0.85	0.83	–	Ref.	5	2	–
	0.1	0.42	0.42	0.43	–	Ref.	1	2	–
Fan-to-ceiling distance (115 rpm, Fan 1)		***0.2 m***	***0.25 m***	***0.3 m***	***0.35 m***	***0.2 m*** *	***0.25m***	***0.3 m***	***0.35 m***
	1.7	1.01	1.01	0.99	0.97	Ref.	0	−2	−4
	1.1	0.94	1.03	1.04	1.08	Ref.	10	11	14
	0.6	0.81	0.93	1.11	0.99	Ref.	14	37	22
	0.1	0.42	0.49	0.44	0.43	Ref.	18	6	3
Ceiling height		***2.5 m***	***3.3 m***	***4 m***	–	***2.5 m*** *	***3.3 m***	***4 m***	–
(115 rpm, Fan 1, 0.3 m fan-to-ceiling distance)	1.7	1.11	1.07	0.91	–	Ref.	−4	−18	–
	1.1	1.12	1.07	0.86	–	Ref.	−4	−23	–
	0.6	1.06	0.85	0.49	–	Ref.	−20	−54	–
	0.1	0.50	0.48	0.19	–	Ref.	−4	−63	–

Note: * Reference condition for the calculation of relative difference.

happens at the 0.6 m height at 0.3 fan-to-ceiling distance. This distance insignificantly influences average air speed at 1.7 m, relative difference smaller than 5%.

4.2. Turbulence kinetic energy (TKE) and turbulence models

Fig. 13 compares the simulated turbulence kinetic energy (TKE) for the height of 1.1 m considering different scenarios. As depicted in Fig. 13a, TKE is increased with the increase of the rotational speed. The highest TKE occurs in the central axis (Y = 0 in Fig. 13) of the fan jet. With regard to the effect of fan blade geometry, Fig. 13b shows that Fan3 creates the lowest level of TKE in Zone 1, directly below the ceiling fan. However, the influence of blade geometry on TKE dampened in the region outside of the fan jet. Generally, the TKE profiles vary primarily in Zone 1 regarding the four investigated factors throughout this study, which is similar to the findings for velocity.

Turbulence and vorticity could be important near fan blade surfaces and tips. Some turbulence models, such as standard k-ω, have advantages to solve boundary layers than k-ε models. SST k-ω model combines k-ω and k-ε models, such that the k-ω is used in the inner region of the boundary layer and switches to the k-ε in the free shear flow.

To further understand how turbulence models influence simulated results, we compared air speeds using five common two-equation turbulence models, standard k-ε, RNG k-ε, realizable k-ε, standard k-ω, and SST k-ω. Fig. 14 shows the comparisons of predicted air speeds at four heights. In general, standard k-ε exhibits slightly better predictions than others when MRF model is applied, but it over-predicts at 0.6 m above the floor. An advanced turbulence model (e.g., LES or DES) might be applied for improvement in the future.

4.3. Comparison with a conceptual fan airflow model

For design purposes, Gao et al. [13] developed a conceptual fan

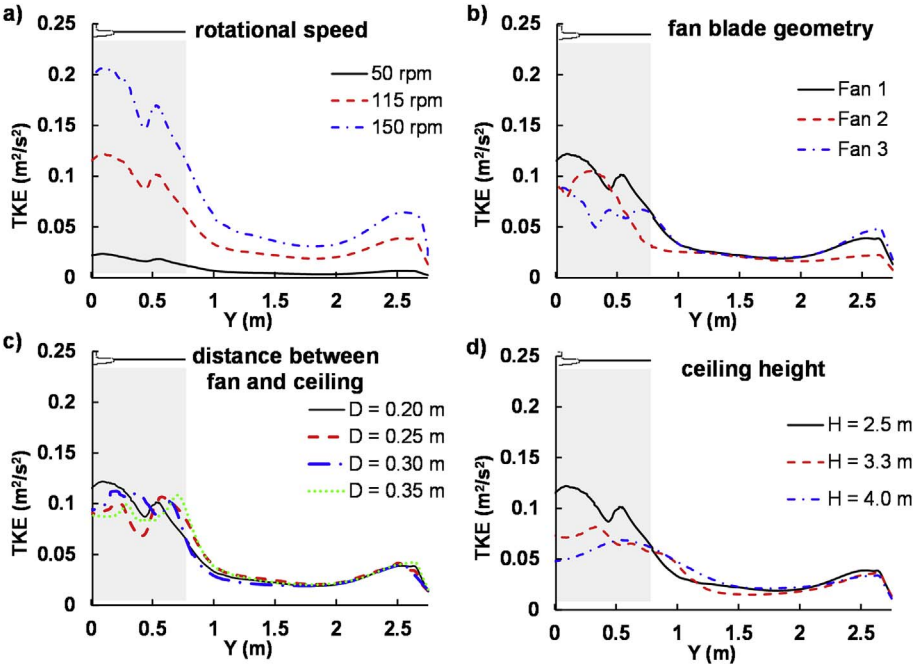

Fig. 13. Comparison of simulated turbulence kinetic energy at the height of 1.1 m with different scenarios: a) rotational speed; b) fan blade geometry; c) distance between fan and ceiling; d) ceiling height (detailed parameter settings can be found in Table 2).

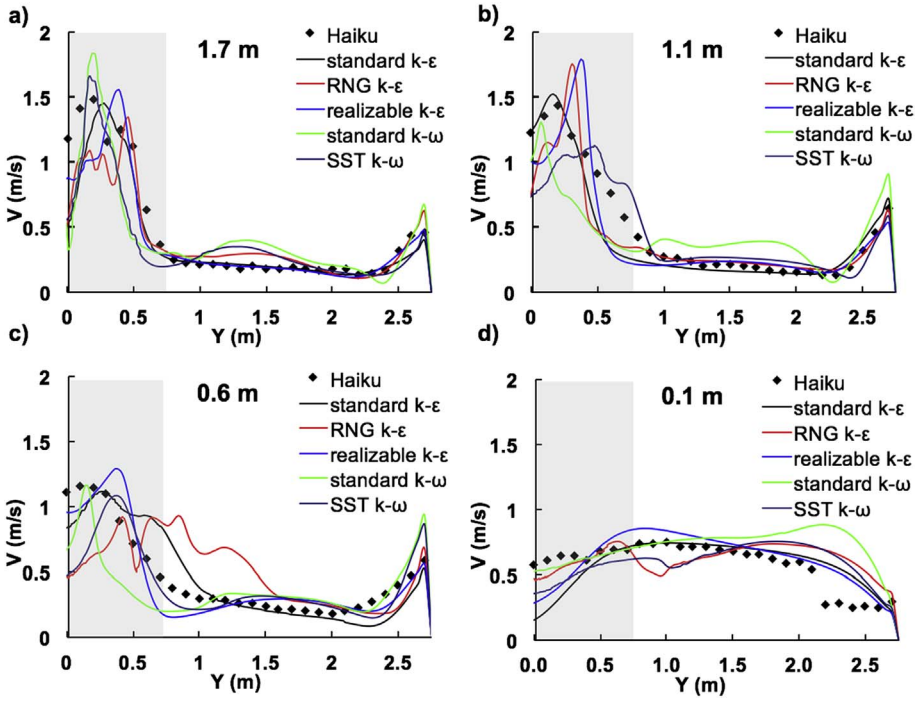

Fig. 14. Comparisons of mean velocity profiles for turbulence models (Fan type: Fan1; Rotational speed: 115 rpm; Ceiling height: 2.5 m; Fan-to-ceiling distance: 0.3 m).

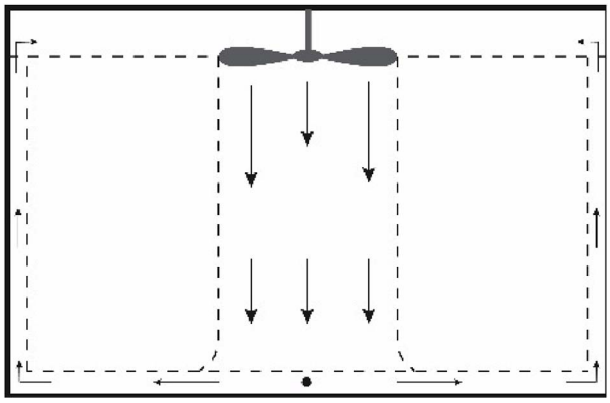

Fig. 15. Conceptual model for a ceiling fan in an unoccupied room [13].

airflow model (Fig. 15) for an unoccupied room. The room with a ceiling fan can be divided into five zones: a fan jet, an impingement zone directly below the fan, a spreading zone of equal thickness across the floor, another set of impingement zones at the base of the walls, and wall zones with upward flow. These zones for airflow patterns can also be found in Figs. 8 and 11 although slight differences in velocity contours exist. Since a ceiling-fan jet is mainly located within a cylindrical zone directly under the fan, however, it is possibly reasonable to simply the fan jet using the conceptual model in Fig. 15 for general indoor thermal environment designs when a detailed airflow pattern is not important.

4.4. Draft potential if ambient temperature not high

In this study, the measured and simulated results (Fig. 6, Fig. 9, Figs. 10 and 12) both show that the highest air speed occurs primarily in the cylindrical zone below a ceiling fan, which is consistent with previous findings [16]. Occupants located directly under a fan are likely to be bothered by draft if the rotational speed is high and the ambient temperature is not very high. A high air speed also exists at lower leg- and ankle-level almost across the whole room. Ankle draft would be a potential risk under cooler ambient conditions, recently assessed in a human subject study [45].

4.5. Limitations

This study has a few limitations. First, the study focuses on an empty room under isothermal conditions. A real room could be much more complex regarding the effects on airflow pattern. Indoor occupancy and furniture would substantially change the results presented in this study. In addition, the fan geometries in this study are rather simple. Ceiling fans with fixtures (e.g., light kits) or other distinctive blade designs (winglets, spikes [24] and fan guard [46], etc.) might result in uncertainties to the presented findings. Furthermore, multiple fans are often applied in larger rooms, such as classroom [14,15]. This study considers only one fan without interaction among multiple fans. Our future studies would address these limitations.

4.6. Other uncertainties

We measured air speed at the steady condition continuously for 3 min. No significant difference was found by measuring air speed for a longer period, such as 5 min and 10 min. Besides, the measurements with omni-anemometers were insufficient to capture airflow directions and other detailed characteristics, such as vortices. Should someone wish to examine this further, particle image velocimetry (PIV) might be applied, as the technique has been used successfully in other indoor environments [47,48].

5. Conclusions

After thorough investigation using experimental tests and CFD simulations, we can draw the following conclusions:

1) Increasing rotational speed of a ceiling fan enhances average air speeds in the occupied zone, especially in the region below the fan blades. Furthermore, velocity profile self-similarity exists for different rotational speeds in the main jet zone below a ceiling fan.
2) Through validation against experimental data, the ceiling fan-driven flow pattern is well predicted by the Standard k-ε turbulence model when incorporated with the Multiple Reference Frame (MRF) fan

model.

3) Both the blade geometry and insufficient distance from fan to ceiling may have significant effect on the velocity distribution in the cylindrical zone below the fan blades. However, the average air speed in the cylindrical zone is only slightly affected, suggesting that the blade geometry is not practically critical in influencing the thermal comfort of occupants. Moreover, similarities of air speed profiles were identified for fans with additional blade shapes and different numbers of blades.
4) For the examined configurations, the rotational speed and ceiling height have a greater effect on the velocity distribution and average air speed in the occupied zone than do the blade geometry and the distance between fan and ceiling.

Acknowledgments

We thank Dr. Baisong Ning for the assistance with laboratory measurement. The CFD work was partially funded by National Key project of the Ministry of Science and Technology, China on Green Buildings and Building Industrialization (Project No. 2016YFC0700501). National Natural Science Foundation of China (Project No. 51308129), and the California Energy Commission Electric Program Investment Change (EPIC) (Project No. EPC-16-013) partially support the experimental work. The authors are also grateful for the financial support from the program of China Sponsorship Council (No. 201706250157) and the Republic of Singapore's National Research Foundation through a grant to the Berkeley Education Alliance for Research in Singapore (BEARS) for the Singapore-Berkeley Building Efficiency and Sustainability in the Tropics (SinBerBEST) Program. BEARS has been established by the University of California, Berkeley as a center for intellectual excellence in research and education in Singapore.

Appendix A. Supplementary data

Supplementary data related to this article can be found at http://dx.doi.org/10.1016/j.buildenv.2017.12.016.

References

[1] S. de la Rue du Can, V. Letschert, M. McNeil, N. Zhou, J. Sathaye, Residential and Transport Energy Use in India: Past Trend and Future Outlook, Ernest Orlando Lawrence Berkeley National Laboratory, Berkeley, CA (US), 2009.
[2] ANSI/ASHRAE/IES Standard 55-2013, Thermal environmental Conditions for Human Occupancy, American Society of Heating, Ventilation, Refrigerating and Air Conditioning Engineers, Atlanta, GA, 2013.
[3] E. Arens, S. Turner, H. Zhang, G. Paliaga, Moving air for comfort, ASHRAE J. 51 (5) (2009) 26–28 18-20,22,24.
[4] Y. Zhai, Y. Zhang, H. Zhang, W. Pasut, E. Arens, Q. Meng, Human comfort and perceived air quality in warm and humid environments with ceiling fans, Build. Environ. 90 (2015) 178–185.
[5] H. Zhang, E. Arens, Y. Zhai, A review of the corrective power of personal comfort systems in non-neutral ambient environments, Build. Environ. 91 (2015) 15–41.
[6] F.H. Rohles, S.A. Konz, B.W. Jones, Enhancing Thermal Comfort with Ceiling Fans, Proceedings of the Human Factors Society 26th Annual Meeting, SAGE Publications Sage CA, Los Angeles, CA, 1982, pp. 118–122.
[7] P.W. James, J.K. Sonne, R.K. Vieira, D.S. Parker, M.T. Anello, Are energy savings due to ceiling fans just hot air, Proceedings of the 1996 ACEEE Summer Study on Energy Efficiency in Buildings, vol. 8, 1996, pp. 89–93 Pacific Grove, CA.
[8] T. Hoyt, E. Arens, H. Zhang, Extending air temperature setpoints: simulated energy savings and design considerations for new and retrofit buildings, Build. Environ. 88 (2015) 89–96.
[9] K. Schmidt, D.J. Patterson, Performance results for a high efficiency tropical ceiling fan and comparisons with conventional fans: demand side management via small appliance efficiency, Renew. Energy 22 (1) (2001) 169–176.
[10] T.U.S.E.P. Agency, ENERGY STAR® Testing Facility Guidance Manual: Building a Testing Facility and Performing the Solid State Test Method for ENERGY STAR Qualified Ceiling Fans, (2002).
[11] S. Schiavon, A.K. Melikov, Energy saving and improved comfort by increased air movement, Energ. Buildings 40 (10) (2008) 1954–1960.
[12] S. Schiavon, A.K. Melikov, Introduction of a cooling-fan efficiency index, HVAC R Res. 15 (6) (2009) 1121–1144.
[13] Y. Gao, H. Zhang, E. Arens, E. Present, B. Ning, Y. Zhai, J. Pantelic, M. Luo, L. Zhao, P. Raftery, S. Liu, Ceiling fan air speeds around desks and office partitions, Build. Environ. 124 (1) (2017) 412–440.
[14] N. Wakamatsu, Y. Momoi, T. Yamanaka, K. Sagara, H. Kotani, Improvement of temperatures stratification caused by air-conditioner by means of ceiling fan in classroom, Proceedings of the 31st AIVC Conference in USB Frash Memory, 2010 Seoul, South Korea.
[15] Y. Momoi, T. Yamanaka, K. Sagara, H. Kotani, N. Wakamatsu, Control of air velocity and temperature distribution in classroom using ceiling fan, Proceedings of the 12th International Conference on Air Distribution in Rooms (ROOMVENT), 2011 Trondheim, Norway.
[16] J.K. Sonne, D.S. Parker, Measured ceiling fan performance and usage patterns: implications for efficiency and comfort improvement, ACEEE Summer Study on Energy Efficiency in Buildings, Cités (1998) 335–341.
[17] R. Aynsley, Fan size and energy efficiency, Int. J. Vent. 1 (1) (2002) 33–38.
[18] S. Zhu, J. Srebric, S.N. Rudnick, R.L. Vincent, E.A. Nardell, Numerical investigation of upper-room UVGI disinfection efficacy in an environmental chamber with a ceiling fan, Photochem. Photobiol. 89 (4) (2013) 782–791.
[19] S. Zhu, J. Srebric, S.N. Rudnick, R.L. Vincent, E.A. Nardell, Numerical modeling of indoor environment with a ceiling fan and an upper-room ultraviolet germicidal irradiation system, Build. Environ. 72 (2014) 116–124.
[20] G. Pichurov, J. Srebric, S. Zhu, R.L. Vincent, P.W. Brickner, S.N. Rudnick, A validated numerical investigation of the ceiling fan's role in the upper-room UVGI efficacy, Build. Environ. 86 (2015) 109–119.
[21] S.N. Rudnick, J.J. McDevitt, G.M. Hunt, M.T. Stawnychy, R.L. Vincent, P.W. Brickner, Influence of ceiling fan's speed and direction on efficacy of upper-room, ultraviolet germicidal irradiation: Experimental, Build. Environ. 92 (2015) 756–763.
[22] E. Adeeb, A. Maqsood, A. Mushtaq, Z. Hussain, Shape optimization of non-linear swept ceiling fan blades through RANS simulations and response surface methods, Proceedings of 12th International Bhurban Conference on Applied Sciences and Technology, IEEE, Islamabad, Pakistan, 2015, pp. 385–390.
[23] M.A. Afaq, A. Maqsood, K. Parvez, A. Mushtaq, Study on the design improvement of an indoor ceiling fan, Proceedings of 11th International Bhurban Conference on Applied Sciences and Technology, IEEE, Islamabad, Pakistan, 2014, pp. 279–283.
[24] A. Jain, R.R. Upadhyay, S. Chandra, M. Saini, S. Kale, Experimental investigation of the flow field of a ceiling fan, ASME 2004 heat transfer/fluids engineering summer conference, Am. Soc. Mech. Eng. (2004) 93–99.
[25] S.J. Volk, Propeller Breeze Enhancing Blades for Conventional Ceiling Fans, (1990) Google Patents.
[26] G.M. Bird, High Efficiency Ceiling Fan, (2004) Google Patents.
[27] D.S. Parker, G.H. Su, B.D. Hibbs, Enhancements to High Efficiency Ceiling Fan, (2005) Google Patents.
[28] D.S. Parker, T. Zambrano, T. Kiceniuk Jr., High Efficiency Twisted Leaf Blade Ceiling Fan, (2008) Google Patents.
[29] D.S. Parker, B. Hibbs, Efficient Traditionally Appearing Ceiling Fan Blades with Aerodynamical Upper Surfaces, (2011) Google Patents.
[30] Y. Momoi, K. Sagara, T. Yamanaka, H. Kotani, Modeling of prescribed velocity generated by ceiling fan based on velocity measurement for CFD simulation, Proceedings of 10th International Conference on Air Distribution in Rooms, 2007, p. 114 Helsinki, Finland.
[31] S. Liu, C. Mak, J. Niu, Numerical evaluation of louver configuration and ventilation strategies for the windcatcher system, Build. Environ. 46 (8) (2011) 1600–1616.
[32] T. Catalina, J. Virgone, F. Kuznik, Evaluation of thermal comfort using combined CFD and experimentation study in a test room equipped with a cooling ceiling, Build. Environ. 44 (8) (2009) 1740–1750.
[33] W. Liu, J. Wen, C.-H. Lin, J. Liu, Z. Long, Q. Chen, Evaluation of various categories of turbulence models for predicting air distribution in an airliner cabin, Build. Environ. 65 (2013) 118–131.
[34] S. Laizet, J. Nedić, C. Vassilicos, Influence of the spatial resolution on fine-scale features in DNS of turbulence generated by a single square grid, Int. J. Comput. Fluid 29 (3–5) (2015) 286–302.
[35] S. Liu, A. Novoselac, Lagrangian particle modeling in the indoor environment: a comparison of RANS and LES turbulence methods (RP-1512), HVAC R Res. 20 (4) (2014) 480–495.
[36] H.-W. Ge, M. Norconk, S.-Y. Lee, J. Naber, S. Wooldridge, J. Yi, PIV measurement and numerical simulation of fan-driven flow in a constant volume combustion vessel, Appl. Therm. Eng. 64 (1–2) (2014) 19–31.
[37] J. Li, Y. Hou, J. Liu, Z. Wang, F. Li, Window purifying ventilator using a cross-flow fan: simulation and optimization, Build. Sci. 9 (4) (2016) 481–488.
[38] F. Babich, M. Cook, D. Loveday, R. Rawal, Y. Shukla, Transient three-dimensional CFD modelling of ceiling fans, Build. Environ. 123 (2017) 37–49.
[39] R. Bassiouny, N.S. Korah, Studying the features of air flow induced by a room ceiling-fan, Energ. Buildings 43 (8) (2011) 1913–1918.
[40] N. Rajaratnam, Turbulent Jets, Elsevier, 1976.
[41] https://grabcad.com/library.
[42] M. Zadravec, S. Basic, M. Hribersek, The influence of rotating domain size in a rotating frame of reference approach for simulation of rotating impeller in a mixing vessel, J. Eng. Sci. Technol. 2 (2) (2007) 126–138.
[43] H.N. Firouz, M.-H. Sarrafzadeh, R. Zarghami, Modelling a multiple reference frame approach in an oxidation ditch of activated sludge wastewater treatment, Frontiers International Conference on Wastewater Treatment and Modelling, vol. 4, Springer, Cham, 2017, pp. 713–717.
[44] S.-T.J. Lien, N.A. Ahmed, Numerical simulation of rooftop ventilator flow, Build. Environ. 45 (8) (2010) 1808–1815.
[45] S. Liu, S. Schiavon, A. Kabanshi, W.W. Nazaroff, Predicted percentage dissatisfied with ankle draft, Indoor Air 27 (4) (2017) 852–862.

[46] S.-C. Lin, M.-Y. Hsieh, An integrated numerical and experimental analysis for enhancing the performance of the hidden ceiling fan, Adv. Mech. Eng. 6 (2014) 214967.
[47] V.A. Reyes, F.Z. Sierra-Espinosa, S.L. Moya, F. Carrillo, Flow field obtained by PIV technique for a scaled building-wind tower model in a wind tunnel, Energy Build. 107 (2015) 424–433.
[48] W. Chen, J. Liu, F. Li, X. Cao, J. Li, X. Zhu, Q. Chen, Ventilation similarity of an aircraft cabin mockup with a real MD-82 commercial airliner, Build. Environ. 111 (2017) 80–90.